Novel Phosphorus-containing Hardeners with Tailored Chemical Structures for Epoxy Resins: Synthesis and Cured Resin Properties

R. M. Perez,[1] J. K. W. Sandler,[1] V. Altstädt,[1] T. Hoffmann,[2] D. Pospiech,[2] J. Artner,[3] M. Ciesielski,[3] M. Döring,[3] A. I. Balabanovich,[4] U. Knoll,[4] U. Braun,[4] B. Schartel[4]

[1]*Department of Polymer Engineering, University of Bayreuth, Universitätsstraße 30, D-95447 Bayreuth, Germany*
[2]*Faculty of Macromolecular Chemistry, Department of Polymer Structures, Leibniz-Institute of Polymer Research Dresden, D-01069 Dresden, Germany*
[3]*Institute of Technical Chemistry, Research Center Karlsruhe GmbH, D-76021 Karlsruhe, Germany*
[4]*Federal Institute for Materials Research and Testing, Unter den Eichen 87, D-12205 Berlin, Germany*

Received 14 November 2006; accepted 19 March 2007
DOI 10.1002/app.26537
Published online 14 May 2007 in Wiley InterScience (www.interscience.wiley.com).

ABSTRACT: A comparative evaluation of systematically tailored chemical structures of various phosphorus-containing aminic hardeners for epoxy resins was carried out. In particular, the effect of the oxidation state of the phosphorus in the hardener molecule on the curing behavior, the mechanical, thermomechanical, and hot-wet properties of a cured bifunctional bisphenol-A based thermoset is discussed. Particular attention is paid to the comparative pyrolysis of neat cured epoxy resins containing phosphine oxide, phosphinate, phosphonate, and phosphate (with a phosphorus content of about 2.6 wt %) and of the fire behavior of their corresponding carbon fiber-reinforced composites. Comparatively faster curing thermosetting system with an enhanced flame retardancy and adequate processing behavior can be formulated by taking advantage of the higher reactivity of the phosphorus-modified hardeners. For example, a combination of the high reactivity and of induced secondary crosslinking reactions leads to a comparatively high T_g when curing the epoxy using a substoichiometric amount of the phosphinate-based hardener. The overall mechanical performance of the materials cured with the phosphorus-containing hardeners is comparable to that of a 4,4′-DDS-cured reference system. While the various phosphorus-containing hardeners in general provide the epoxy-based matrix with enhanced flame retardancy properties, it is the flame inhibition in the gas phase especially that determines the improvement in fire retardancy of carbon fiber-reinforced composites. In summary, the present study provides an important contribution towards developing a better understanding of the potential use of such phosphorus-containing compounds to provide the composite matrix with sufficient flame retardancy while simultaneously maintaining its overall mechanical performance on a suitable level. © 2007 Wiley Periodicals, Inc. J Appl Polym Sci 105: 2744–2759, 2007

Key words: flame retardance; organo-phosphorus compounds; fracture toughness

INTRODUCTION

Epoxy-based resins are commonly used for applications including adhesives, insulating materials for electrical devices as well as for advanced fiber-reinforced composites in the transportation sector. By accident or deliberately, these products can be exposed to either local ignition sources or, in the worst case, a postcrash fire scenario. Owing to environmental concerns and varying qualification requirements, both the flammability and the toxicological consequences of combustion of flame-retardant epoxy resins have recently become a subject of considerable attention.[1] Many approaches have been taken to improve the thermal stability and flame retardancy of epoxy resins using either nonreactive or reactive flame retardants.[1–8] Nonreactive flame retardants are widely used because of the comparative ease of promoting flame retardancy to polymeric materials. However, there are several disadvantages associated with common additives such as poor compatibility, migration, and a severe reduction of the mechanical properties of the final product.[9,10] To overcome these disadvantages and to meet the newly arising environmental regulations, standards, and test methods, the currently emerging chemistry is aimed at developing and employing novel halogen-free flame retardants tailored for a specific system and/or application.

Some of the most widely used flame retardants are phosphorus-containing compounds. With a con-

Correspondence to: V. Altstädt (altstaedt@uni-bayreuth.de).

Contract grant sponsor: German Research Foundation (DFG); contract grant numbers: AL474/3-1, AL474/4-1, PO 575/5-1/8-1, SCHA 730/6-1, DO 453/4-1/4-2.

sumption growth rate of 7% per year, phosphorus-based compounds will become the third-most important flame retardant additive.[11] Many studies[2,4–7,12–21] have indeed shown that a high degree of flame retardancy and thermal stability can be imparted to an epoxy resin by the use of phosphorus compounds. A common strategy to increase the flame retardancy of an epoxy resin matrix is the addition of reactive (a curing agent for example) or nonreactive organo-phosphorus compounds.[12,15,17] In this regard, it was recently demonstrated that the ease of processability and the resulting mechanical properties of carbon fiber-reinforced composites can be maintained on a high level by employing up to 20 wt % of nonreactive 9,10-dihydro-9-oxa-10-phosphaphenanthrene-10-oxide (DOPO)-based compounds ($\sim$ 2 wt % of phosphorus).[22,23] However, the final matrix material still showed a moderate decrease of the glass transition temperature, a common feature for such additive-modified epoxies.

Unlike nonreactive organo-phosphorus additives, phosphorus-containing amines used as curing agents are covalently bonded to the epoxy network overcoming the disadvantages outlined above. Furthermore, the chemical structure of the amine can be tailored to increase the amount of phosphorus in the resulting material and, subsequently, a further addition of other additives for improving the flame retardancy (reactive or nonreactive) can be avoided. More importantly, given that the phosphorus-containing units are structurally fixed in the polymer, volatile products do not appear to form during combustion.[24] This observation in turn implies that the eco-toxicological impact of the material upon burning can be significantly reduced.

With the main focus on the curing reaction, the flame retardancy, and the thermal stability, several studies have verified that triaryl phosphine oxide[7,20,25–29] or DOPO-based[30–32] aminic hardeners can be used as curing agents for epoxy resins. However, only a few studies[7,20,26] attempted to carry out a systematic tailoring of the chemical structures of such curing agents. Furthermore, little efforts have as yet been devoted towards understanding how the curing behavior, the fracture toughness, or the moisture absorption of the resulting materials are affected when using such tailored curing agents. In addition, the application of such compounds to the manufacture of fiber-reinforced materials and the assessment of their resulting physical and mechanical properties which will ultimately define the usefulness of such compounds as an effective source of flame retardancy for modern-day composites has not yet been evaluated.

As the flame retardant potential of various phosphorus-modified aminic hardeners in general has been highlighted in previous studies, the present study was aimed at presenting a systematic evaluation of the effect of various phosphorus-containing aminic hardeners with tailored chemical structures on the curing behavior and the subsequent solid-state properties of a difunctional epoxy matrix. Four phosphorus-containing aromatic diaminic hardeners that differ with respect to the number of oxygen atoms linked to the phosphorus atom were synthesized and used to cure a diglycidyl ether of bisphenol A (DGEBA). For comparison, the epoxy resin was also cured with 4,4′-diamino diphenyl sulfone (4,4′-DDS).

The effects of the different hardeners on the curing behavior, the thermal stability, water uptake as well as the dynamic mechanical properties and fracture toughness of the cured epoxy were examined and the observed variations in properties were correlated with changes in the structure of the epoxy network. Lastly, the potential of these curing agents as flame retardants for modern carbon fiber-reinforced composites is addressed.

MATERIALS AND EXPERIMENTAL DETAILS

A difunctional epoxy resin (DGEBA, Ruetapox 0162) with an epoxy equivalent weight of 173 g/equiv which is free of hydroxyl groups was supplied by Bakelite (Iserlohn, Germany) and was used as received. The 4,4′-DDS (control hardener), with an amine equivalent weight of 62 g/equiv, was purchased from Merck (synthesis grade, Darmstadt, Germany) and used as received. Four phosphorus-containing aminic hardeners, namely bis(3-aminophenyl)phenyl phosphine oxide (PO) (**1**), bis(3-aminophenyl) phosphinic acid phenylester (PO2) (**2**), phenylphosphonic acid bis(3-aminophenyl)ester (PO3) (**3**), and phosphoric acid bis(3-aminophenyl)ester phenylester (PO4) (**4**) were synthesized in the laboratory according to the procedures described in the latter section, with a purity exceeding 98% as determined by means of NMR spectra. The PO, PO2, PO3, and PO4 hardeners have phosphorus contents of 10.1, 9.6, 9.1, and 8.7 wt %, respectively. An overview of the chemical structures of the compounds employed in this study is given in Scheme 1.

It is worth mentioning that, owing to the electron-withdrawing and, therefore, meta-guiding effects of the aromatic phosphorus group in electrophilic aromatic substitution, only the synthesis of *meta*-PO and *meta*-PO2 can be accomplished in a justifiable manner. Hence, for comparative purposes, compounds PO3 and PO4 were also synthesized with the amine in meta position, in spite of the considerably higher price of *meta*-nitrophenol as compared with its regio-isomers.

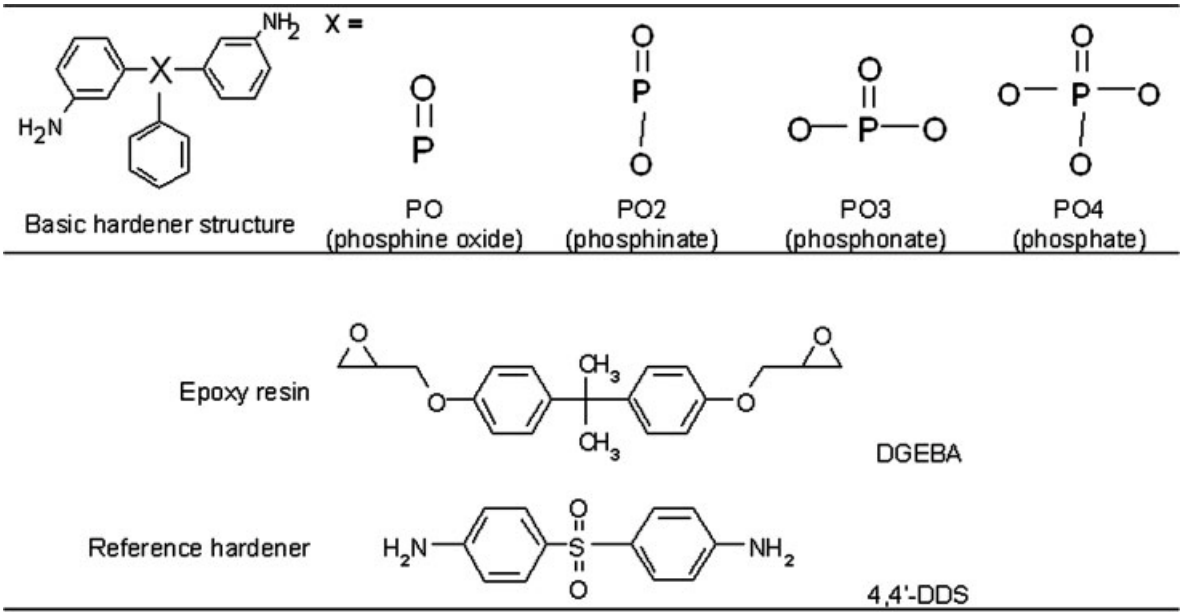

Scheme 1 Overview of the chemical structures of the materials used in this study.

Synthesis of the phosphorus-containing aminic hardeners (Scheme 2)

Compounds (**1**) (PO) and (**5**) were prepared according to an approach by Liu et al.,[20] starting from triphenylphosphine oxide by nitration in sulfuric acid and fuming nitric acid and a successive reduction using tin(II)chloride and hydrochloric acid, with a yield of 70 and 90%, respectively. Phosphinic acid (6) was synthesized by simultaneous hydrolisation, oxidation and nitration of chlorodiphenylphosphine in sulfuric acid and fuming nitric acid, with a yield of 74%.[33,34] The acid was esterifies with phenol via an intermediate acid chloride made in refluxing thionylchloride, with an overall yield of 74%.[35] The nitroester (**7**) was hydrated by Pd/C and hydrogen to give diamine (**2**) (PO2) with a yield of 82%. For the esterification of phenylphosphonic acid dichloride and phenylphosphoric acid dichloride with *m*-nitrophenol to give compounds (**8**) and (**9**), the method of Liu et al.[20]—used for the synthesis of phenylphosphonic acid bis(4-nitrophenyl)ester—was adapted. The substances were obtained with a yield of 82 and 73%, respectively, and were hydrated by Pd/C and hydrogen to give diamines (**3**) (PO3) and (**4**) (PO4) with a yield of 91 and 76%, respectively.

Infrared spectra (IR) were obtained using a Perkin–Elmer System 2000 FT-IR spectrophotometer. Nuclear magnetic resonance (''NMR'') spectra were recorded using a Bruker AC-250 with tetramethylsilane and trimethylphosphate[36] as internal standards. Elemental analysis was performed using a Vario EL III from Elementar Analysensysteme GmbH. High-resolution mass spectrometry (''HRMS'') and electron impact mass spectrometry (''MS'') were performed using a Finnigan MAT-4000-1. Melting points were obtained using a Büchi B-545 at a heating rate of 3°C/min.

Chlorodiphenylphosphine, phenylphosphonic acid dichloride, phenylphosphoric acid dichloride (ABCR), absolute tetrahydrofuran (''THF_{abs}''), 10 wt % of palladium on charcoal (''Pd/C''), phenol, *m*-nitrophenol, thionylchloride (Fluka), triethylamine 99.5% (''TEA''), and copper(I)chloride (Aldrich) were used as received. Hydrogen 5.0 was provided by Basi.

Reactions with Pd/C and H_2 were performed in a 1-L steel autoclave equipped with a thermocouple, a Brooks 5866 pressure controller and a Bronkhorst F-231C-FD-33-V flow regulator.

Bis-(3-nitrophenyl) phosphinic acid (**6**)

For 30 min, chlorodiphenylphosphine (95 wt %, 125 g, 0.54 mol) and then, for another 30 min, 25 mL water are added to 250 mL ice-cold concentrated sulfuric acid under major evolution of heat and hydrogen chloride. Fuming nitric acid (250 mL) was added dropwise over a period of 4 h while maintaining a temperature of less than 20°C by using an ice-bath. The solution was slowly warmed, stirred overnight at room temperature, and finally poured on ice. The precipitate was filtered off, washed with water, and air-dried. Recrystallization from acetic acid produced white crystals with a purity exceeding 98%. Yield: 123 g (74%). Mp: ≈ 265°C (Decomp.; Lit: 268°C,[33] 268–270°C.[34] $Anal_{found}$: C, 46.75; H, 3.00; N, 9.03. $Anal_{calc}$ ($C_{12}H_9N_2PO_6$): C, 46.77; H, 2.94; N, 9.09. HRMS: M_{found} = 308.0207, M_{calc} = 308.0198. MS (70 eV): *m/z* = 308, 291, 262, 246, 216. IR (KBr): 1609, 1534, 1420, 1351, 1285, 1150 cm^{-1}. ^1H NMR (d_6-DMSO):

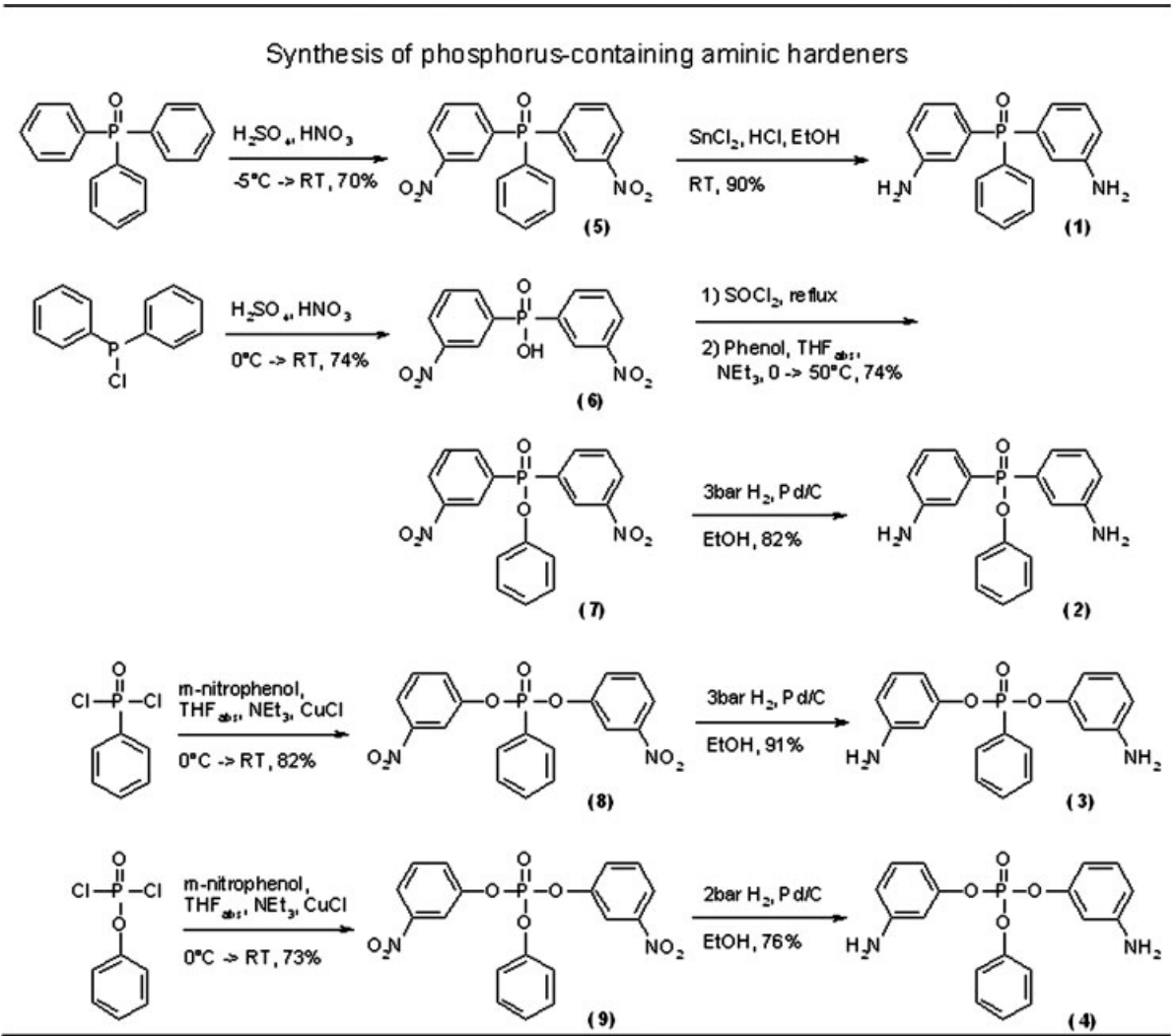

Scheme 2 Overview of the synthesis pathways for the phosphorus-containing hardeners.

δH = 7.78 (ddd, 2H, J_{PH} = 3.1 Hz, J_{HH1} = 7.2 Hz, J_{HH2} = 8.1 Hz, N—C—CH—C*H*), 8.19 (dd, 2H, J_{PH} = 11.2 Hz, J_{HH1} = 7.2 Hz, P—C—C*H*—CH), 8.37 (d, 2H, J_{HH2} = 8.1 Hz, *N*—C—C*H*—CH), 8.52 (d, 2H, J_{PH} = 12.6 Hz, C—CH—C), 12.40 (bs, 1H, OH) ppm. ^{13}C NMR (d_6-DMSO): δC = 125.4 (J_{CP} = 11.5 Hz, C—CH—C), 126.5 (J_{CP} = 2.3 Hz, N—C—*C*H—CH), 130.6 (J_{CP} = 13.2 Hz, N—C—CH—CH), 137.0 (J_{CP} = 136.1 Hz, C—P), 137.4 (J_{CP} = 10.3 Hz, P—C—CH—CH), 147.7 (J_{CP} = 15.5 Hz, N—C) ppm. ^{31}P NMR (d_6-DMSO): δP = 18.2 ppm.

Bis-(3-nitrophenyl) phosphinic acid phenylester (**7**)

A suspension of (**6**) (92.5 g, 0.3 mol) and thionylchloride (110 mL, 1.5 mol) was refluxed overnight under exclusion of moisture. Thionylchloride was distilled off, the remaining solid was grounded and added to 300 mL THF_{abs} at 80°C under an argon atmosphere. The suspension was cooled in an ice-bath and during the 1 h, phenol (31.1 g, 0.33 mol) and TEA (46 mL, 0.33 mol), dissolved in 200 mL THF_{abs}, were added. Afterwards, the reaction mixture was stirred at 50°C for 3 h. Precipitated triethylamine hydrochloride was filtered off and extracted with THF. The concentrated filtrate was diluted with 700-mL ice-cold $CHCl_3$, washed thrice with 300 mL of 2 wt % ice-cold aquatic NaOH solution and thrice with 300 mL of water, and was dried over Na_2SO_4. Recrystallization from EtOH produced white crystals with a purity exceeding 98%. Yield: 85.2 g (74%). M_p: 114°C. $Anal_{found}$: C, 56.38; H, 3.80; N, 7.01. $Anal_{calc}$ ($C_{18}H_{13}N_2PO_6$): C, 56.26; H, 3.41; N, 7.29. HRMS: M_{found} = 384.0426, M_{calc} = 384.0511. MS (70eV): *m/z* = 384, 383, 367, 337, 291, 245. IR (KBr): 1608, 1540, 1528, 1487, 1351, 1249, 1195, 1090 cm^{-1}. ^{1}H NMR ($CDCl_3$): δH = 7.07 (t, 1H, J_{HH1} = 7.1 Hz, *p*-Ph), 7.10–7.26 (m, 4H, *o*-Ph and *m*-Ph), 7.67 (ddd, 2H, J_{PH} = 3.6 Hz, J_{HH2} = 7.6 Hz, J_{HH3} = 8.3 Hz,

N—C—CH—C*H*), 8.19 (dd, 2H, J_{PH} = 11.9 Hz, J_{HH2} = 7.6 Hz, P—C—C*H*—CH), 8.35 (d, 2H, J_{HH3} = 8.3 Hz, N—C—C*H*—CH), 8.67 (d, 2H, J_{PH} = 13.2 Hz, C—CH—C) ppm. ^{13}C NMR ($CDCl_3$): δC = 120.6 (J_{CP} = 4.6 Hz, *o*-Ph), 125.7 (*p*-Ph), 126.8 (J_{CP} = 12.2 Hz, C—*C*H—C), 127.8 (J_{CP} = 2.7 Hz, N—C—*C*H—CH), 130.3 (*m*-Ph), 130.6 (J_{CP} = 13.8 Hz, N—C—CH—*C*H), 132.6 (J_{CP} = 140.7 Hz, C—P), 137.6 (J_{CP} = 10.2 Hz, P—C—*C*H—CH), 148.4 (J_{CP} = 16.4 Hz, N—C), 150.1 (J_{CP} = 7.9 Hz, O—C) ppm. ^{31}P NMR ($CDCl_3$): δP = 24.1 ppm.

Bis-(3-aminophenyl) phosphinic acid phenylester (**2**)

Compound (**7**) (57.6 g, 0.15 mol) was dissolved in 700 mL hot EtOH and 1 g Pd/C was added to the solution. The reaction mixture was kept at 45°C and 3 bar H_2 with strong stirring until no further consumption of H_2 was detected. Pd/C was filtered off and EtOH was removed by vacuum distillation. Recrystallization from CH_2Cl_2 produced pale yellow crystals with a purity exceeding 98%. Yield: 39.9 g (82%). M_p: 125°C. $Anal_{found}$: C, 66.59; H, 5.59; N, 8.65. $Anal_{calc}$ ($C_{18}H_{17}N_2PO_2$): C, 66.66; H, 5.28; N, 8.64. HRMS: M_{found} = 324.0960, M_{calc} = 324.1028. MS (70eV): *m/z* = 324, 323, 231. IR (KBr): 1630, 1596, 1487, 1441, 1312, 1280, 1199, 1108 cm^{-1}. ^{1}H NMR ($CDCl_3$): δH = 3.77 (bs, 4H, NH), 6.70 (d, 2H, J_{HH1} = 7.4 Hz, N—C—C*H*—CH), 6.98 (t, 1H, J_{HH2} = 6.9 Hz, *p*-Ph), 7.08–7.21 (m, 10H) ppm. ^{13}C NMR ($CDCl_3$): δC = 117.5 (J_{CP} = 11.7 Hz, C—*C*H—C), 118.6 (J_{CP} = 2.7 Hz, N—C—*C*H—CH), 120.6 (J_{CP} = 4.8 Hz, *o*-Ph), 121.1 (J_{CP} = 10.0 Hz, P—C—*C*H—CH), 124.3 (*p*-Ph), 129.3 (J_{CP} = 14.9 Hz, N—C—CH—*C*H), 129.4 (*m*-Ph), 131.6 (J_{CP} = 137.1 Hz, C—P), 146.7 (J_{CP} = 16.0 Hz, N—C), 150.9 (J_{CP} = 8.3 Hz, O—C) ppm. ^{31}P NMR ($CDCl_3$): δP = 32.0 ppm.

Phenylphosphonic acid bis-(3-nitrophenyl)ester (**8**)

m-Nitrophenol (104.3 g, 0.75 mol), TEA (104 mL, 0.75 mol) and 1 g of CuCl were dissolved in 450 mL THF_{abs} under an argon atmosphere. The solution was cooled in an ice-bath and during the 2 h, phenylphosphonic acid dichloride (95 wt %, 71.8 g, 0.35 mol), dissolved in 250 mL THF_{abs}, was added dropwise and, afterwards, the reaction stirred for another 3 h at room temperature. Precipitated triethylamine hydrochloride was filtered off and was extracted with THF. The concentrated filtrate was diluted with 750 mL ice-cold $CHCl_3$ and was washed twice with 250 mL of 3 wt % ice-cold aquatic NaOH solution. The combined aquatic solutions were extracted with 100 mL $CHCl_3$ and the combined organic solutions were washed thrice with 200 mL water and were dried over Na_2SO_4. Recrystallization from EtOH produced white crystals with a purity exceeding 98%. Yield: 115.3 g (82%). Mp: 91°C. $Anal_{found}$: C, 54.03; H, 3.25; N, 6.92. $Anal_{calc}$ ($C_{18}H_{13}N_2PO_7$): C, 54.01; H, 3.27; N, 7.00. HRMS: M_{found} = 400.0485, M_{calc} = 400.0460. MS (70eV): *m/z* = 400, 399, 383, 262. IR (KBr): 1534, 1473, 1442, 1346, 1271, 1206, 1131, 1079 cm^{-1}. ^{1}H NMR ($CDCl_3$): δH = 7.51–7.83 (m, 7H, O—C—C*H*—CH and *m*-Ph and *N*—C—CH—C*H* and *p*-Ph), 8.00–8.22 (m, 6H, C—CH—C and *N*—C—C*H*—CH and *o*-Ph) ppm. ^{13}C NMR ($CDCl_3$): δC = 115.8 (J_{CP} = 5.1 Hz, C—*C*H—C), 120.2 (*N*—C—*C*H—CH), 124.5 (J_{CP} = 193.0 Hz, C—P), 126.7 (J_{CP} = 4.4 Hz, O—C—*C*H—CH), 128.9 (J_{CP} = 16.2 Hz, *m*-Ph), 130.5 (*N*—C—CH—*C*H), 132.0 (J_{CP} = 10.9 Hz, *o*-Ph), 134.1 (J_{CP} = 3.2 Hz, *p*-Ph), 148.6 (*N*—C), 150.0 (J_{CP} = 7.3 Hz, O—C) ppm. ^{31}P NMR ($CDCl_3$): δP = 14.2 ppm.

Phenylphosphonic acid bis-(3-aminophenyl)ester (**3**)

Compound (**8**) (56.0 g, 0.14 mol) was dissolved in 750 mL hot EtOH and 1 g of Pd/C was added to the solution. The reaction mixture was kept at 40°C and 3 bar H_2 with strong stirring until no further consumption of H_2 was detected. Pd/C was filtered off and EtOH was removed by vacuum distillation. Recrystallization from CH_2Cl_2 produced reddish crystals with a purity exceeding 98%. Yield: 43.5 g (91%). *Mp*: 116°C. $Anal_{found}$: C, 63.42; H, 5.30; N, 8.16. $Anal_{calc}$ ($C_{18}H_{17}N_2PO_3$): C, 63.53; H, 5.04; N, 8.23. HRMS: M_{found} = 340.0970, M_{calc} = 340.0977. MS (70eV): *m/z* = 340, 232, 200. IR (KBr): 1628, 1577, 1493, 1465, 1440, 1249, 1141 cm^{-1}. ^{1}H NMR ($CDCl_3$): δH = 3.61 (bs, 4H, NH), 6.43 (d, 2H, J_{HH1} = 8.2 Hz, N—C—C*H*—CH), 6.52 (d, 2H, J_{HH2} = 7.4 Hz, O—C—C*H*—CH), 6.54 (s, 2H, C—CH—C), 7.03 (dd, 2H, J_{HH1} = 8.2 Hz, J_{HH2} = 7.4Hz, N—C—CH—C*H*), 7.41–7.53 (m, 2H, *m*-Ph), 7.58 (t, 1H, J_{HH3} = 7.4 Hz, *p*-Ph), 7.93 (dd, 2H, J_{PH} = 13.9 Hz, J_{HH4} = 7.7 Hz, *o*-Ph) ppm. ^{13}C NMR ($CDCl_3$): δC = 107.2 (J_{CP} = 4.6 Hz, C—CH—C), 110.2 (J_{CP} = 4.7 Hz, O—C—*C*H—CH), 111.8 (N—C—*C*H—CH), 127.0 (J_{CP} = 193 Hz, C—P), 128.5 (J_{CP} = 15.9 Hz, *m*-Ph), 130.1 (N—C—CH—*C*H), 132.2 (J_{CP} = 10.3 Hz, *o*-Ph), 133.0 (J_{CP} = 3.2 Hz, *p*-Ph), 147.9 (*N*—C), 151.3 (J_{CP} = 7.7 Hz, O—C) ppm. ^{31}P NMR ($CDCl_3$): δP = 11.8 ppm.

Phosphoric acid bis-(3-nitrophenyl)ester phenylester (**9**)

m-Nitrophenol (73.7 g, 0.53 mol), TEA (74 mL, 0.53 mol), and 1 g of CuCl were dissolved in 200 mL THF_{abs} under an argon atmosphere. The solution was cooled in an ice bath and during the 1 h, phenylphosphoric acid dichloride (52.7 g, 0.25 mol)

dissolved in 125 mL THF_{abs}, was added dropwise and, afterwards, the reaction was stirred for another 2 h at room temperature. Precipitated triethylamine hydrochloride was filtered off and was extracted with THF. The concentrated filtrate was diluted with 600-mL ice-cold CH_2Cl_2 and was washed twice with 200 mL of 2 wt % ice-cold aquatic NaOH solution. The combined aquatic solutions were extracted with 100 mL CH_2Cl_2 and the combined organic solutions were washed with 200 mL water and were dried over Na_2SO_4. Recrystallization from MeOH produced white crystals with a purity exceeding 98%. Yield: 76.2 g (73%). M_p: 61°C. $Anal_{found}$: C, 51.98; H, 3.07; N, 7.01. $Anal_{calc}$ ($C_{18}H_{13}N_2PO_8$): C, 51.93; H, 3.15; N, 6.73. HRMS: M_{found} = 416.0398, M_{calc} = 416.0410. MS (70eV): *m/z* = 416, 399, 371, 324. IR (KBr): 1589, 1533, 1477, 1349, 1294, 1204, 1183, 1082 cm^{-1}. ^1H NMR ($CDCl_3$): δH = 7.12–7.24 (m, 3H, *o*-Ph and *p*-Ph), 7.32 (dd, 2H, $J_{HH1} \approx (J_{HH2} \approx$ (7.7 Hz, *m*-Ph), 7.44–7.61 (m, 4H, N—C—CH—CH—C*H* and N—C— CH—C*H*), 7.95–8.11 (m, 4H, C—CH—C and N— C—C*H*—CH) ppm. ^{13}C NMR ($CDCl_3$): δC = 115.7 (J_{CP} = 5.6 Hz, C—*C*H—C), 119.9 (J_{CP} = 4.9 Hz, *o*-Ph), 120.9 (N—C—*C*H—CH), 126.3 (J_{CP} = 4.7 Hz, N—C—CH—CH—*C*H), 126.4 (*p*-Ph), 130.2 (*m*-Ph), 130.8 (N—C—CH—*C*H), 149.0 (N—C), 149.7 (J_{CP} = 7.6 Hz, O—*C*—CH—CH—CH—CH), 150.3 (J_{CP} = 6.8 Hz, O—*C*—CH—C) ppm. ^{31}P NMR ($CDCl_3$): δP: −17.6 ppm.

Phosphoric acid bis-(3-aminophenyl)ester phenylester (**4**)

Compound (**9**) (41.6 g, 0.1 mol) was dissolved in 250 mL hot EtOH and 1 g of Pd/C was added to the solution. The reaction mixture was kept at 30°C and 2 bar H_2 with strong stirring until no further consumption of H_2 was detected. Pd/C was filtered off, the EtOH was removed by vacuum distillation and the remaining substance was dissolved in 150 mL CH_2Cl_2. The formed precipitate was filtered off and CH_2Cl_2 was removed by vacuum distillation. Recrystallization from EtOH produced reddish crystals with a purity exceeding 98%. Yield: 27.1 g (76%). Mp: 112°C. $Anal_{found}$: C, 60.94; H, 5.12; N, 7.81. $Anal_{calc}$ ($C_{18}H_{17}N_2PO_4$): C, 60.68; H, 4.81; N, 7.86. HRMS: M_{found} = 356.0921, M_{calc} = 356.0926. MS (70eV): *m/z* = 356, 262, 247, 200. IR (KBr): 1611, 1585, 1492, 1467, 1276, 1207, 1167, 1141 cm^{-1}. ^1H NMR ($CDCl_3$): δH = 3.65 (bs, 4H, NH), 6.37 (d, 2H, J_{HH1} = 7.9 Hz, *N*—C—C*H*—CH), 6.44 (s, 2H, C—CH—C), 6.50 (d, 2H, J_{HH2} = 8.2 Hz, N—C—CH—CH—C*H*), 6.97 (dd, 2H, J_{HH1} = 7.9 Hz, J_{HH2} = 8.2 Hz, N—C—CH—C*H*), 7.05–7.18 (m, 3H, *o*-Ph and *p*-Ph), 7.26 (dd, 2H, $J_{HH3} \approx (J_{HH4} \approx$ (7.9 Hz, *m*-Ph) ppm. ^{13}C NMR ($CDCl_3$): δC = 106.5 (J_{CP} = 5.1 Hz, N—C—*C*H—C), 109.4 (J_{CP} = 5.0 Hz, N—C—CH—CH—*C*H), 112.1 (N—C—*C*H—CH), 120.1 (J_{CP} = 4.8 Hz, *o*-Ph), 125.4 (*p*-Ph), 129.7 (*m*-Ph), 130.2 (N—C—CH—*C*H), 148.1 (N—C), 150.4 (J_{CP} = 7.7 Hz, O—*C*—CH—CH—CH—CH), 151.2 (J_{CP} = 7.2 Hz, O—*C*—CH—C) ppm. ^{31}P NMR ($CDCl_3$): δP = −17.9 ppm.

Preparation of the resin systems

The DGEBA was placed in a glass flask and was heated to 80–90°C in an oil bath connected to a temperature controller. The desired amount of phosphorus-containing hardener was then added slowly to the resin and was mixed with a mechanical stirrer for 30 min at 600–1000 rpm, keeping the temperature constant at 80–90°C, until the compound was dissolved and the mixture was clear. The ratio of epoxy-amine equivalent was adjusted between 0.8 and 1.2. The hot mixture was then poured into a preheated aluminum mold at 80°C and was placed in a vacuum oven at the same temperature for 30 min for degassing. Some amount of these mixtures was immediately stored in a refrigerator at −20°C for the DSC measurements.

The phosphorus-containing epoxy resin was then cured as follows: the curing cycle started by a 2 K/min ramp from room temperature to 180°C. This temperature was held for 2 h and curing was completed with a −2 K/min ramp from 180°C to room temperature. For easy release of the cured epoxy resin sheets, the mold surface was coated with a thin layer of Frekote-700 NC.

Thus, a 110 × 110 × 4 mm^3 epoxy resin sheet was obtained and was subsequently machined to the desired specimen size for further testing. Control samples of DGEBA cured with a substoichiometric amount of DDS (1 : 0.8) were prepared following a similar procedure, the mixing temperature was 130°C.

Preparation of composites

Composite plates of 400 × 400 × 2.8 mm^3 containing 60 vol % of carbon fibers were manufactured using the resin transfer molding (RTM) or hand lay-up technique in the case of the epoxy cured with PO. The phosphorus-containing matrices were prepared as described in the previous section. Following this procedure, the hot mixture was placed in a vacuum oven at 80°C for 30 min for degassing. The fiber reinforcement consisted of eight plies of woven fabric (Atlas 1/4, 5 harness satin, ECC GmbH and CO, fiber aerial weight = 370 g/m^2) that were placed in the preheated RTM mold at 80–100°C. The resin mixtures were preheated to the same temperature and driven into the closed RTM mold by vacuum, followed by curing at 180°C for 2 h and a slow cooling to room temperature. For easy release

of the cured composite plate, the mold surface was coated with a thin layer of Frekote-700 NC. A composite reference based on the reference epoxy matrix (DGEBA/DDS) was prepared under identical conditions.

Curing behavior

The kinetics of the curing reaction were determined by means of isothermal differential scanning calorimetry (DSC) experiments performed using a thermal analysis DCSQ1000 from TA Instruments with 6.0 ± 0.5 mg of uncured material under a nitrogen atmosphere (50 mL/min). The calorimeter was preheated to the desired temperature (120–200°C) before the unreacted sample was placed in the calorimeter cell and the heat flow was immediately recorded as a function of the time after the sample was inserted. The beginning of the curing reaction was taken as the time when the ratio between the temperature change of the cell and the steady-state value was less than 0.01. Thus, the reaction was assumed to be under isothermal conditions after about the first minute. The cure under isothermal conditions was considered to be completed after 240 min or when the heat flow signal reached steady-state conditions. The final steady-state of the heat flow signal was taken as the base line. Following the isothermal step, the sample was cooled to room temperature at 10 K/min, followed by a temperature ramp from 25 to 300°C at the same heating rate to determine the glass transition temperature (T_g). Crimped aluminum pans were used for all DSC measurements.

Thermomechanical properties of the cured samples

Dynamic mechanical analysis (DMA) was performed using a RDAIII from Rheometric Scientific at a heating rate of 4 K/min from 25 to 250°C. A cured rectangular specimen of 50 × 10 × 3 mm^3 was used in the torsion rectangular geometry mode, at a frequency of 1 Hz and 0.1% of deformation. The glass transition temperature (T_g) was taken as the temperature at which tan δ showed a maximum.

To measure the glass transition temperature of conditioned samples, dry rectangular specimens with the dimensions of 50 × 10 × 3 mm^3 were immersed in distilled water at a constant temperature of 70°C for 14 days. Following the conditioning, DMA experiments were performed using identical experimental conditions as for the dry samples.

Water absorption of the cured samples

The moisture uptake of the epoxy cured with the various hardeners was studied as a function of the time. For each epoxy formulation, three specimens of a length of 30 mm, a width of 15 mm, and a thickness of 1–1.5 mm were prepared. This comparatively small specimen thickness was chosen to allow a one-dimensional diffusion process neglecting edge effects. Following a drying step in vacuum at 60°C for 24 h, the samples were weighted and immersed in distilled water at temperatures of 50, 70, and 90°C, respectively. The moisture absorption as a function of the immersion time was measured by weighting the specimens periodically until equilibrium was eventually reached. The results presented correspond to the average weight gain of the three specimens.

The normalized water uptake during immersion (W_t) was calculated according to

$$W_t = \left(\frac{m_t - m_0}{m_0}\right) \times 100, \quad (1)$$

where m_0 and m_t are the weight of the dry and wet specimen at time t, respectively. Assuming a Fickian diffusion process, the moisture absorption as a function of time can be written as[37]

$$\frac{W_t}{W_\infty} = 1 - \exp\left[-7.3 \cdot \left(\frac{Dt}{b^2}\right)^{0.75}\right], \quad (2)$$

where W_∞ is the moisture absorption at equilibrium and b is the specimen thickness. The diffusion constant (D) was obtained from the initial slope of the W_t versus $t^{1/2}$ plot given by

$$D = \left(\left(\frac{d(W_t)}{dt^{1/2}}\right)_{t\to 0} \frac{b}{4 \cdot W_\infty}\right)^2 \pi. \quad (3)$$

Mechanical properties of the cured samples

The critical stress intensity factor (K_{Ic}) and the fracture mechanical modulus were obtained from the opening mode test according to the ISO 13,586, performed on compact tension (CT) specimens. The size of the specimens used in this study was 41 × 40 × 4 mm^3. A sharp V-notch was machined into the specimens and then a sharp precrack was generated by tapping a razor blade. Tests were carried out using a universal testing machine model Zwick Z 2.5 at room temperature and a cross-head speed of 10 mm/min. A minimum of four specimens for each epoxy formulation were tested.

Thermal stability of the cured samples

The thermal stability of the various cured epoxy formulations was investigated by thermogravimetric (TG) experiments using a TGA/SDTA 851 (Mettler/Toledo, Gießen, Germany), applying a nitrogen flow

of 30 mL/min. The samples (about 10 mg) were heated in alumina pans from room temperature up to about 927°C at a heating rate of 10 K/min.

Flammability of carbon fiber-reinforced composites

The limited oxygen index (LOI) of the prepared carbon fiber-reinforced composites with various matrix systems was determined according to ISO 4589 (specimen size: 6 × 3 × 100 mm^3) and the UL94 classification (specimen size: 13 × 3 × 125 mm^3) was determined according to ISO 1210.

The fire behavior of the composites for flaming conditions was characterized using a cone calorimeter (Fire Testing Technology, East Grinstead, UK) according to ISO 5660 (sample size: 100 × 100 × 3 mm^3) in the horizontal position using a retainer frame with a heat flux of 35 kW/m^2. If the reproducibility was satisfactorily, the measurements were done only in duplicate, if not, triple measurements were carried out.

RESULTS AND DISCUSSION

In the present study we are able to present, in view of the intended purpose, justifiable synthesis pathways to yield three novel phosphorus-based diamines (PO2, PO3, and PO4) with an excellent purity. In comparison to the compound PO, the reduction of the nitro-group in case of the other hardeners was carried out with hydrogen under pressure; however, this particular synthesis step might eventually impose problems related to legal and engineering aspects. In addition, the compound PO2 had to be synthesized in three steps; as such, using one step more as compared to all the other hardeners. As far as adequate equipment is available, up-scaling the synthesis to obtain larger amounts of the materials for more detailed investigations does not pose a significant challenge. Nevertheless, the complexity of the synthesis of such phosphorus-containing compounds should always be considered in the context of the resulting material and its final physical and mechanical properties.

All the phosphorus-modified hardeners but the PO were completely soluble in the DGEBA at the studied epoxy-amine ratios. The mixtures were still liquid but were highly viscous at room temperature, with a viscosity ranging from 11 to 1000 Pa s depending on the formulation. Nevertheless, the cured epoxy sheets were clear, yellow to orange in color, and were optically homogeneous and transparent.

Curing behavior

The curing kinetics of the different thermosetting systems were comparatively evaluated for the stoichiometric formulations under isothermal conditions. To estimate the rate of the reaction (dx/dt) and the epoxy conversion (x), two assumptions have to be made: (i) the epoxy curing reaction is a thermal event only and (ii) the heat flow obtained from the DSC (dq/dt) is proportional to the reaction rate (dx/dt).[38] Thus, the reaction rate at any time t is given by the heat flow divided by the overall heat of reaction (ΔH_0)

$$\frac{dx}{dt} = \frac{1}{\Delta H_0}\frac{dq}{dt}. \tag{4}$$

The epoxy conversion (or the degree of cure) at a time t for any formulation is obtained by integration of eq. (4)

$$x(t) = \frac{1}{\Delta H_0}\int_0^t \frac{dq}{dt}dt. \tag{5}$$

The overall heat of reaction, ΔH_0, was taken as the total heat evolved from the reaction of the epoxy formulation obtained from an isothermal DSC measurement at 200°C. The heat of reaction was found to vary between 105 and 114 kJ/equiv for the various systems, which is in very good agreement with the values reported for a full cure of stoichiometric mixtures.[38–40]

A comparative plot of the rate of reaction for all different epoxy formulations as a function of the epoxy conversion at 180°C is shown in Figure 1(a), whereas a more detailed insight into the rate of reaction at various temperatures as a function of the epoxy conversion is highlighted in Figure 1(b) for the DGEBA-PO3 system. Typical characteristics of autocatalytic reaction mechanisms such as an initial nonzero rate of reaction (when $x \rightarrow 0$) and a maximum in the rate of reaction can clearly be observed for all epoxy formulations. The autocatalytic reaction mechanism of epoxy-amine systems has been extensively reported in the literature[38,41–43] and is considered for modeling the curing reaction.[44–47] When curing a thermoset without a catalyst, the reaction of a primary amine with an epoxy results in a secondary amine. Subsequently, the reaction is autocatalyzed by the formed hydroxyl groups.

As shown in Figure 1(a), the initial and the maximum rate of reaction are generally higher for the epoxy cured with the phosphorus-modified hardeners as compared with the DDS. The initial reaction rate can be ordered as PO > PO2 > PO3 > PO4 > DDS. This effect can be ascribed to the different electron withdrawing strength of the —P=O as compared with the SO_2 group. The SO_2 group shows a stronger electron withdrawing strength than the —P=O group; hence, the nucleophilicity of the amine is significantly reduced. This observation is in good

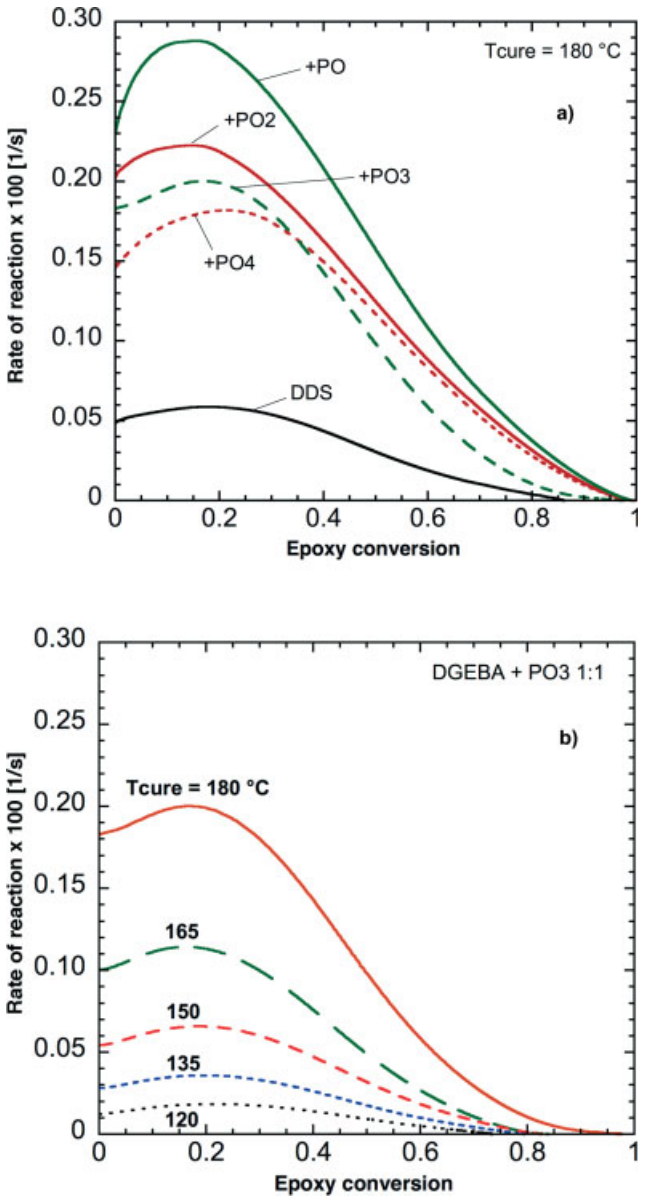

Figure 1 Isothermal DSC scans of epoxy resin formulations cured with (a) different phosphorus-containing hardeners at 180°C, and (b) PO3 at various temperatures. [Color figure can be viewed in the online issue, which is available at www.interscience.wiley.com.]

agreement with various earlier studies[7,20] indicating a higher nucleophilicity of the amine in hardener molecules containing the —P=O group. On the other hand, given the similarity of the amines equivalent weights, similar amounts of epoxy (66–69 wt %) were needed to prepare the mixtures. Therefore, in the present case, the nucleophilicity of the amine is the major factor expected to influence the curing reaction (at least in the case of PO2, PO3, and PO4) rather than diffusion processes.[48]

Not unexpectedly, an increase in the rate of the reaction and a shift of the maximum rate to lower conversions with increasing temperature is also observed for the epoxy cured with PO3, Figure 1(b). The final conversion attained when curing the epoxy with PO3 at $T < 180$°C was less than 85%. This effect can be explained by the curing reaction taking place under diffusion-control when curing below 180°C for $\sim$ 240 min. Thus, after gelation, the system vitrifies and the molecular mobility is significantly reduced which, in turn, decreases the rate of the epoxy conversion. A similar behavior is observed for any epoxy-amine system when curing at a temperature below the corresponding maximum achievable glass transition temperature.

The relative reactivity of the different hardeners in terms of the primary amine-epoxy reaction can also be established by comparing the time to reach gelation.[42,49] According to Flory's theory of gelation,[50] the conversion at gelation is constant and independent of temperature, given that the network structure is a function of the conversion only. The conversion at gelation can be calculated as

$$x_{\text{gel}} = \left(\frac{r}{(f_e - 1)(f_a - 1)}\right)^{0.5}, \qquad (6)$$

where r is the epoxy-amine stoichiometric ratio and f_e and f_a are the epoxy and amine functionalities, respectively. For the studied systems, $f_e = 2$ and $f_a = 4$; thus, for a stoichiometric mixture $x_{\text{gel}} \approx 0.58$. The time to reach x_{gel} is summarized in the Table I for the different epoxy-amine formulations cured at various temperatures. On the basis of these results it can be concluded that the relative reactivity of the different hardeners follows the trend of PO > PO2 > PO3 $\sim$ PO4 > DDS. On the contrary, a slightly higher reactivity has been assigned to a phenylphosphonic acid bis(4-aminophenyl)ester hardener (similar to PO3) in the literature[20] as compared with a bis(3-aminophenyl) phenyl phosphine oxide hardener (comparable to PO in this study). This apparent disagreement is most likely related the different

TABLE I
Time to Reach Conversion at Gel (x_{gel}) for the Different Epoxy-Amine Formulations Cured at Various Temperatures

	Time to reach x_{gel} = 0.58 (s)				
	T_{cure} (°C)				
Hardener	120	150	165	180	200
DDS	21,600	4280	2271	1316	659
PO	–	1543	640	265	149
PO2	4319	1098	684	336	203
PO3	4622	1302	783	400	245
PO4	4498	1120	768	389	238

The epoxy-amine equivalent ratio is 1 : 1.

position of the amino-group for the phenylphosphonic acid bis(4-aminophenyl)ester as compared with the PO3 hardener. Hence, both steric hindrance and electronic effects are influencing the reactivity of the hardeners.

The dependence of the glass transition temperature of all studied epoxy formulations on the stoichiometric amount of amine is summarized in Figure 2. The epoxy formulations were cured for 240 min at a sufficiently high temperature so that the glass transition temperature shown in Figure 2 represents the maximum achievable (not affected by neither vitrification nor thermal degradation). The highest crosslinking density of any network is achieved at the stoichiometric epoxy-amine ratio. In agreement with most studies in the literature based on DGEBA,[40,51,52] a maximum in the glass transition temperature was attained at a 1 : 1 epoxy-amine ratio for any amine, as shown in Figure 2.

In agreement with theoretical predictions using statistical methods,[51] the change in T_g with increasing stoichiometric ratio is larger for an epoxy excess as compared with an amine excess. However, the PO2-cured epoxy deviates from this general trend; most likely due to the occurrence of side reactions such as etherification which create a higher number of crosslink points in this particular network. The higher reactivity of the PO2 as compared with the other studied amines and the excess of epoxy present in the mixture appear to have encouraged further crosslinking reactions which, in turn, resulted in the particularly high glass transition temperature observed at the substoichiometric composition.

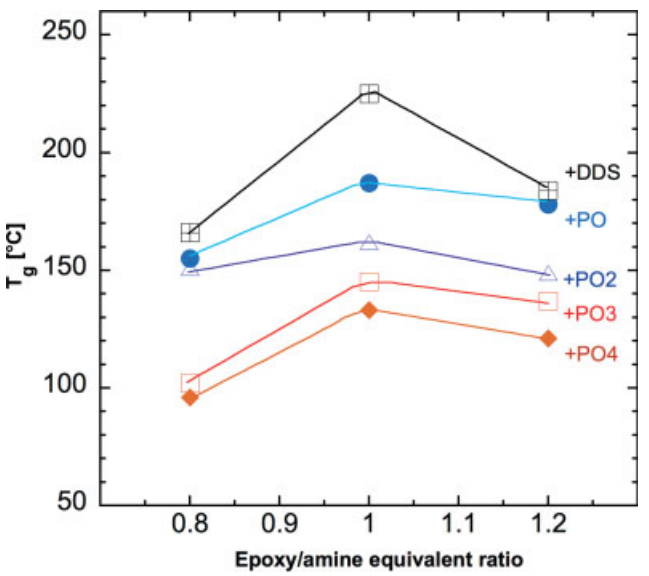

Figure 2 Glass transition temperature of the different epoxy formulations as a function of the epoxy-amine ratio. [Color figure can be viewed in the online issue, which is available at www.interscience.wiley.com.]

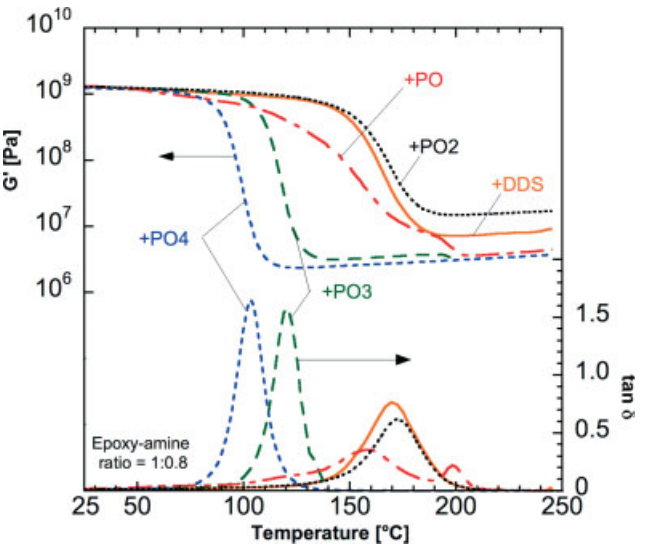

Figure 3 Results of the dynamic mechanical analysis of the epoxy cured with different phosphorus-containing hardeners. [Color figure can be viewed in the online issue, which is available at www.interscience.wiley.com.]

This experimental result suggests that the optimum T_g will not necessarily be attained at the stoichiometric epoxy-amine ratio, in agreement with other studies.[40,53,54] A combination of a higher amine reactivity and a substoichiometric amine to epoxy ratio would lead to better properties of the final material as other studies have shown that unreacted amines decrease the mechanical properties and increase the water absorption.[53]

DMA results of the cured epoxy formulations

The storage modulus and tan δ of the cured epoxy resin formulations with a substoichiometric amount of the different hardeners are summarized in Figure 3 as a function of the temperature. As can be seen, at 25°C, the storage modulus of the phosphorus-modified systems is maintained on a similar level as that of the DDS-cured reference, independent of the chemical structure of the hardener used to cure the epoxy.

In the rubbery region, the storage modulus decreases in the order of PO2 > DDS > PO > PO3 > PO4. Only the system cured with the PO-hardener shows a different modulus behavior, revealing two transitions at around 160 and 200°C. This phenomenon can, again, be attributed to the incomplete dissolution of this hardener as discussed before and the subsequent further curing reaction during the DMA experiment. In fact, this system appears to reach an ultimate glass transition temperature of about 200°C, as indicated by the second peak in the tan δ curve. Consequently, owing to these reasons,

the data for the epoxy cured with PO is excluded from the following analysis.

The trend in glass transition temperature of the different systems, as given by the peak position of tan δ in Figure 3, can be explained in terms of their corresponding crosslinking density. According to the theory of rubber elasticity,[55,56] the crosslinking density is proportional to the storage modulus at T_g + 45 K; in turn, a higher crosslinking density implies stronger restrictions to molecular motions and, thus, a higher T_g.

A consistent correlation between the rubbery modulus and the glass transition temperature can be observed for the epoxy cured with DDS, PO3, and PO4. However, the epoxy cured with PO2 does not follow this trend. Employing a statistical approach,[51] the theoretical average molecular weight between crosslinks (M_c) for the epoxy cured with PO2 is estimated as 843 g/mol; however, experimentally one finds M_c = 318 g/mol. The occurrence of secondary crosslinking side reactions in this system can explain the higher rubbery modulus and the achieved high glass transition temperature, in agreement with the results obtained by the DSC measurements.

The magnitude and shape of the tan δ peak of the epoxy cured with PO3 is comparable to that of the epoxy cured with PO4, indicating similar network structures and, thus, similar damping properties of the two systems. This observation is not surprising, given the similarity of the chemical structures of the hardeners. An analogous argument follows for the epoxy cured with DDS and PO2.

Water uptake of the cured epoxy formulations

Representative plots of the water uptake as a function of time of the epoxy cured with DDS at various immersion temperatures and of the epoxy cured with the different phosphorus-modified hardeners at a fixed immersion temperature of 70°C are shown in Figures 4(a,b), respectively. The solid lines indicate theoretical predictions based on a Fickian behavior as given by eq. (2).

As shown in Figure 4(a), there generally is an increase in the initial rate of diffusion (proportional to the initial slope of the curve) of the DDS-cured epoxy with increasing immersion temperature, indicating the thermally-activated nature of the water absorption process. Whereas the samples conditioned at 50°C appear to reach saturation, the materials do not reach equilibrium at higher temperatures and the uptake deviates significantly from the Fickian behavior. This observation can be in part attributed to the relative proximity of the immersion temperature to the glass transition temperature of this wet epoxy system (wet T_g = 142°C as determined by DMA). Hence, viscoelastic effects would

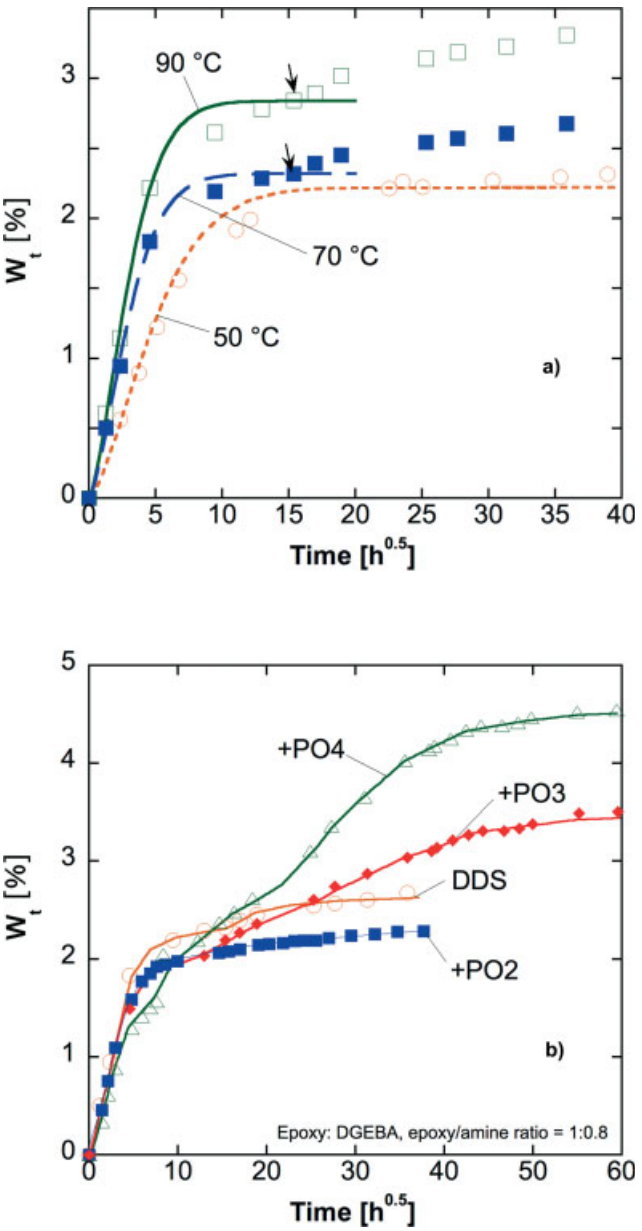

Figure 4 Water uptake as a function of $t^{1/2}$ of epoxy resin formulations cured with (a) DDS at various immersion temperatures, and (b) different phosphorus-containing hardeners at an immersion temperature of 70°C. [Color figure can be viewed in the online issue, which is available at www.interscience.wiley.com.]

contribute to an enhanced water transport into the network, in agreement with previous studies in the literature.[37,57,58] It is worth mentioning at this point that an ''initial saturation'' value (as indicated by the arrows) was used to fit the experimental water absorption data using Fick's law; therefore, ''apparent'' diffusion coefficients are calculated and are summarized in Table II.

The glass transition temperature of the wet samples was determined by means of DMA after 14

TABLE II
Glass Transition Temperatures of the Dry and Conditioned Epoxy Samples Cured with Different Phosphorus-Containing Hardeners

				D (cm^2/s) $\times 10^9$		
		T_g wet (°C)		T (°C)		
Hardener	T_g dry (°C)	1st trans.	2nd trans.	50	70	90
DDS	170	142	171	6.31	16.49	17.78
PO2	172	140	162	–	18.48	–
PO3	121	96	120	–	13.28	–
PO4	103	82	104	–	10.94	–

The moisture diffusion coefficients obtained for each system from the Fick's law are also included. The epoxy-amine equivalent ratio is 1 : 0.8.

days of immersion, the results are summarized in Table II. Given that these samples were conditioned up to the onset of the beginning of the second-phase absorption (time ~18 h$^{0.5}$), single hydrogen bonds with the epoxy network are expected to be the dominant form of the absorbed water.[59] Two major transition temperatures were observed in the tan δ curves and are summarized in Table II: a transition at low temperatures attributed to the plasticizing effect of the absorbed water,[10,59] and a transition which occurs after the water is removed from the epoxy at high temperatures during the experiment. This second transition temperature agrees well with the T_g of the dry samples, indicating that the absorbed water has been completely removed.

The effect of the type of hardener on the water uptake at 70°C of the cured epoxy is presented in Figure 4(b). As shown, the initial rate of water absorption is hardly influenced by the chemical structure of the hardener. On the other hand, neither of the studied systems seems to reach an equilibrium water uptake under the selected experimental conditions and the deviation from the Fickian behavior is clearly seen for all systems. As discussed before, an apparent diffusion coefficient is estimated by considering the ''initial saturation'' at $t \sim 16$ h$^{0.5}$ as an equilibrium level.

The data shown in Figure 4(b) also highlight that, up to the ''initial saturation'' level (time ~ 18 h$^{0.5}$), the water uptake behavior is fairly similar for all studied systems; however, beyond this initial saturation, a marked difference in the absorption is observed. The epoxy cured with DDS or PO2 only shows a slight deviation from the Fickian behavior, whereas a more pronounced deviation is seen for the epoxy cured with PO3 or PO4. The different behaviors can be correlated with a combined effect of (i) the proximity of the immersion temperature to the wet glass transition temperature (ΔT), (ii) the crosslinking density of the systems, and (iii) the oxidation of the resin.

It is noted that ΔT is larger for the epoxy cured with DDS or PO2 ($\Delta T \sim 100$°C) than for the epoxy cured with PO3 or PO4 ($\Delta T \sim 30$–50°C). Thus, in the latter case, a higher extend of polymer relaxation is believed to enhance the water absorption in these systems.[60] In addition, owing to the lower crosslinking density of these resins (more ''open'' network), the hydrophilic sites are more available for water absorption. On the other hand, the color change of the materials observed during the experiment indicates that an oxidative process of the resins might also have occurred; hence, the oxidized resin was more prone to absorb water. This observation agrees with similar results reported in the literature for an epoxy-amine system.[60]

Fracture toughness of the cured epoxy formulations

The effect of the chemical structure of the hardener on the fracture mechanical properties of the resulting materials was determined for the epoxy cured with a substoichiometric amount of DDS, PO2, and PO3. The fracture toughness and fracture mechanical modulus of the representative systems measured at room temperature are summarized in Table III.

The data presented in Table III reveals a direct correlation between the fracture toughness and the M_c of the studied materials. This observation indicates that the brittleness of the resulting material is related to its crosslinking density, in agreement with

TABLE III
Fracture Toughness, Fracture Mechanical Modulus, and Experimental Molecular Weight between Crosslinks of the Epoxy Formulations with Different Phosphorus-Containing Hardeners at Room Temperature

Hardener	K_{IC} (MPa m$^{0.5}$)	E-modulus[a] (GPa)	M_{Cexp} (g/mol)
DDS	0.56 ± 0.04	3.8 ± 0.3	643
PO2	0.44 ± 0.01	3.9 ± 0.2	318
PO3	0.67 ± 0.06	3.8 ± 0.4	1450

The epoxy-amine equivalent ratio is 1 : 0.8.
[a] obtained from the initial slope of the stress-strain data from the K_{IC} evaluation.

TABLE IV
TG Results of Neat Cured Resins

Hardener	DDS	PO	PO2	PO3	PO4
Main decomposition step					
ΔT (°C)	377–457	364–447	331–402	327–387	324–377
ΔWt (%)	78.8 ± 1	64.7 ± 1	54.7 ± 1	51.7 ± 1	51.1 ± 1
T_{max} (°C)	405 ± 2	414 ± 2	355 ± 2	348 ± 2	345 ± 2
Subsequent decomposition step					
ΔT (°C)	457–527	447–527	402–527	387–527	377–527
Wt (%)	3.6 ± 1	12.0 ± 1	16.3 ± 1	16.7 ± 1	14.2 ± 1
Following decomposition of the residue					
ΔT (°C)	527–902	527–902	527–902	527–902	527–902
ΔWt (%)	3.2 ± 1	4.1 ± 1	5.0 ± 1	5.3 ± 1	5.9 ± 1
Residue at 902°C					
Wt (%)	14.4 ± 1	19.2 ± 1	24.0 ± 1	27.3 ± 1	29.8 ± 1

Heating rate 10 K/min[1]; ΔT, temperature range; T_{max}, temperature at maximum mass loss.

several previous studies. As the average molecular weight between crosslinks increases, the ability of the resulting material to deform plastically increases as well. Thus, a larger deformation zone is formed ahead of the crack tip for materials with a larger M_c. This effect, in turn, contributes to a comparatively large amount of energy absorption during fracture for the epoxy cured with PO3; hence, higher fracture toughness was observed for this system.

The modulus values reported in Table III were estimated from the slope of the load-displacement curve obtained when measuring the fracture toughness of the specimens. The influence of the chemical structure of the hardener is, within experimental error, hardly reflected in these modulus values. On the other hand, the experimental approach in itself might in part explain the low sensivity with regard to the corresponding M_c. Nevertheless, the general trend of the modulus values presented in Table III is consistent with that observed in the DMA experiments at room temperature.

Thermal stability of the cured epoxy formulations

A comprehensive investigation of the pyrolysis of the cured epoxy formulations to establish the decomposition pathways using TG, TG-evolved gas analysis, FTIR of the residue, kinetics, XPS, etc., is exceeding the scope of this article and is described elsewhere.[61] Only the main decomposition characteristics of the various epoxy formulations are summarized in Table IV and are discussed here to complete the picture.

All materials are characterized by a main and a subsequent decomposition step, followed by a high-temperature decomposition of the residue. The mass loss of the epoxy cured with DDS is dominated by a main decomposition step (79 wt %), whereas the second decomposition step is only of minor importance (3.6 wt %). In contrast, the mass loss during the main decomposition step of the epoxy cured with the phosphorus-containing hardeners decreased to about 51–64 wt % and the mass loss during the second decomposition step increased to about 12–17 wt %. The following high-temperature decomposition behavior is similar for all materials.

The high-temperature residue increases in the order of DDS < PO < PO2 < PO3 < PO4. Additional analytical investigations verified that the amount of phosphorus remaining in the residue also increased and the amount of phosphorus released to the gas phase decreased in the same order, respectively.[61] The decomposition temperature of the main decomposition step was significantly decreased ($\Delta T = \sim 50$–60°C) for the epoxy cured with PO2, PO3, and PO4, whereas it remained nearly unchanged for the epoxy cured with PO. These results regarding the thermal stability agree well with results published for phosphine oxide, phosphonate, and phosphate structures previously used in epoxy resins.[62–69]

Flammability of the corresponding carbon fiber-reinforced composites

A comprehensive evaluation of the flammability, the fire behavior, and the fire retardancy mechanisms of the carbon fiber-reinforced composites (fiber content 60 vol %) based on the epoxy resin cured with the different hardeners described in this study is published elsewhere.[61] Yet, some of the main results are summarized in Table V to highlight the potential of the evaluated hardeners as an effective approach towards achieving advanced materials that do not only show a suitable processibility and mechanical behavior but also reasonable flame retardancy. Composites based on the epoxy cured with DDS were used as a reference to assess the flammability

TABLE V
Ignition, Flammability (LOI, UL 94), and Fire Behavior of Fiber-Reinforced Composites

Hardener	DDS	PO	PO2	PO3	PO4
t_{ig} (s)	122 ± 2	79 ± 10	105 ± 5	106 ± 3	107 ± 1
LOI (%)	31 ± 1	39 ± 1	34 ± 1	36 ± 1	29 ± 1
UL 94	HB	V-1	HB	HB	HB
Peak HRR (kW/m^2)	322 ± 30	240 ± 30	355 ± 30	450 ± 30	525 ± 30
THE (MJ/m^2)	23.3 ± 3.0	25.0 ± 3.0	21.5 ± 3.0	23.2 ± 3.0	21.6 ± 3.0

t_{ig}, peak HRR, and THE from cone calorimeter investigations at 35 kW/m^2.

and fire performance of composites based on the epoxy cured with PO, PO2, PO3, and PO4. However, it should be noted that the epoxy cured with DDS does not allow for a systematic comparison, as the additional SO_2 group has a significant impact on charring and fuel dilution.

The time to ignition (t_{ig}) obtained in the cone calorimeter experiments can be ordered as PO < PO2 = PO3 = PO4 ≤ DDS, a trend that corresponds well to the decomposition temperatures obtained by TG, apart for the composite based on the epoxy cured with PO. This deviation might be partly due to the hand lay-up technique applied. The flammability behavior in terms of LOI is ordered as PO > PO3 ≥ PO2 > DDS > PO4. Only the composite based on the epoxy cured with PO showed a LOI value approaching 40 and, thus, showed self extinguishing behavior in the UL 94 test. The performance under flaming condition was characterized by the peak of heat release rate (peak HRR) and the total heat evolved (THE). The peak HRR is ordered with increasing fire risk as PO < PO2 = DDS < PO3 = PO4, whereas the THE did not show significant differences with respect to the data error. The reason for the latter result was the high fiber content resulting in a minor importance of charring by the epoxy resin and, hence, of flame retardancy mechanisms being active in the condensed phase. The heat release per mass loss was obtained in the order of DDS = PO4 < PO3 = PO2 < PO. This result correlates well with the phosphorus vaporization potential observed by the thermal analysis and the performance in terms of flammability and fire behavior. It became clear, that flame inhibition plays the major role to improve the fire retardancy in fiber-reinforced composites. Thus, only the epoxy cured with PO displayed a convincing fire retardancy effect.

CONCLUSIONS

A systematic tailoring of the chemical structure of various phosphorus-containing aminic hardeners for epoxy resins was carried out. The molecular tailoring was aimed at delivering an understanding of the influence of the oxidation state of the phosphorus (in the hardener molecule) on the liquid-state and solid-state properties of a bisphenol-A based thermosetting system. However, this study was not only focused on the synthesis of such compounds but, more importantly, on the curing behavior, the thermomechanical, and mechanical as well as the hot/wet properties of the resulting phosphorus-containing thermoset. Special emphasis was placed on the pyrolysis of neat cured epoxy resins and the fire behavior of their corresponding carbon fiber-reinforced composites.

Four different phosphorus-containing (phosphine oxide (PO), phosphinate (PO2), phosphonate (PO3), and phosphate (PO4)-based) hardeners were synthesized and were employed at varying stoichiometric ratios to cure a diglycidyl ether of bisphenol-A. The resulting phosphorus content in any of the phosphorus-containing epoxy matrices was about 2.6 wt %. Apart from the PO, neither of the hardeners posed any difficulties with regard to the processability of neat and fiber-reinforced materials.

The relative reactivity of the hardeners was found to correlate with the oxidation state of the phosphorus in the hardener molecule (PO > PO2 > PO3 ~ PO4 > DDS). Both steric hindrance and electronic effects influence the reactivity of the hardeners. On the basis of these results, the possibility of controlling the rate of reaction of thermosetting systems by mixing various hardeners and, in turn, optimizing the processing times for liquid composite molding technologies for fiber-reinforced materials become apparent.

In general, the glass transition temperature (T_g) of the phosphorus-modified epoxy networks also correlated well with the oxidation state of the phosphorus in the hardener molecule; indeed, the relative order of T_g of the cured epoxy networks was PO > PO2 > PO3 > PO4. The oxygen atoms linked to the benzene ring in the PO3 or PO4 molecules act as ''spacers,'' providing the corresponding networks with a greater flexibility than their analogue molecules, i.e., PO and PO2, respectively. This observation was further verified by the similarity of the tan δ curves of the PO and PO2 or the PO3 and PO4-

cured epoxies (similar networks). As expected, the maximum T_g of either network was achieved at the stoichiometric epoxy-amine composition; however, in the case of the epoxy cured with a substoichiometric amount of PO2, a combined high reactivity and the occurrence of secondary crosslinking reactions led to a comparatively high T_g.

No detrimental effects were observed on the mechanical properties of the cured neat resins. Indeed, the room temperature stiffness of the epoxy cured with the phosphorus-containing hardeners was maintained on a level similar to that of the epoxy cured with 4,4′-DDS and the fracture toughness of some of the phosphorus-containing materials was higher than that of the epoxy cured with 4,4′-DDS. It becomes apparent from these results that the oxidation state of the phosphorus in the hardener molecule not only influences the fire behavior of the material but also the ability of the epoxy network to withstand a larger plastic deformation through the M_c increase.

The fire behavior of the fiber-reinforced composites was influenced by a combined condensed and gas phase mechanism. Although an increase in the condensed phase-action of phosphorus with an increasing oxidation of the phosphorus was found, the flame inhibition with decreasing oxidation state in the gas phase appeared to be dominant. Differences in the charring of the materials had only a minor influence on the fire behavior of the composites. Thus, contrary to the expectations, only the composite containing the phosphine oxide (PO)-based matrix showed an enhanced performance in terms of flammability (UL 94, LOI) and fire behavior (cone calorimeter).

In summary, the fire performance of organophosphorus modified epoxy thermosets is not necessarily determined by the presence of a phosphorus-containing compound only; crucial in this regard is the way in which the phosphorus interacts with its surroundings. More importantly, a good balance must exist between the ease of processing, the kinetics of the curing reaction, the overall physical and mechanical performance of the neat thermosetting matrix and the flammability and fire behavior of the reinforced material. This balance, in turn, is what will ultimately decide the potential use of such phosphorus-containing compounds for demanding future applications.

References

1. Lu, S. J.; Hamerton, I. Prog Polym Sci 2002, 27, 1661.
2. Kim, J.; Yoo, S.; Bae, J. Y.; Yun, H. C.; Hwang, J.; Kong, B. S. Polym Degrad Stab 2003, 81, 207.
3. Lengsfeld, H.; Altstädt, V. Kunststoffe 2001, 91, 94.
4. Shieh, J. Y.; Wang, C. S. J Appl Polym Sci 2000, 78, 1636.
5. Lji, M.; Kiuchi, Y. Polym Adv Technol 2001, 12, 393.
6. Wang, C. S.; Lin, C. H. J Appl Polym Sci 2000, 75, 429.
7. Jain, P.; Choudhary, V.; Varma, I. K. J Therm Anal Calorim 2002, 67, 761.
8. Xiao, W.; He, P.; He, B. J Appl Polym Sci 2002, 86, 2530.
9. Troitzsch, J. International Plastics Flammability Handbook; Hanser: Münich, 1990.
10. Shaw, S. J. In Chemistry and Technology of Epoxy Resins; Ellis, B., Ed.; Blackie Academic: London, 1993; Chapter 4.
11. Murphy, J. Plast Additives Compounding, 1999, 1, 20.
12. Jeng, R. J.; Shau, S. M.; Lin, J. J.; Su, W. C.; Chiu, Y. S. Eur Polym J 2002, 38, 683.
13. Shieh, J. Y.; Wang, C. S. J Polym Sci Part A: Polym Chem 2002, 40, 369.
14. Lin, C. H.; Wang, C. S. Polymer 2001, 42, 1869.
15. Hussain, M.; Varley, R. J.; Mathus, M.; Burchill, P.; Simon, G. P. J Mater Sci Lett 2003, 22, 455.
16. Shieh, J. Y.; Wang, C. S. Polymer 2001, 42, 7617.
17. Wang, C. S.; Lin, C. H. J Polym Sci Part A: Polym Chem 1999, 37, 3903.
18. Liu, Y. L. Polymer 2001, 42, 3445.
19. Hörold, S. Polym Degrad Stab 1999, 64, 427.
20. Liu, Y. L.; Hsiue, G. H.; Lee, R. H.; Chiu, Y. S. J Appl Polym Sci 1997, 63, 895.
21. Wu, C. S.; Liu, Y. L.; Chiu, Y. C.; Chiu, Y. S. Polym Degrad Stab 2002, 78, 41.
22. Perez, R.; Sandler, J. K. W.; Altstädt, V.; Hoffmann, T.; Pospiech, D.; Ciesielski, M.; Döring, M. J Mater Sci 2006, 41, 341.
23. Perez, R. M.; Sandler, J. K. W.; Altstädt, V.; Hoffmann, T.; Pospiech, D.; Ciesielski, M.; Döring, M.; Braun, U.; Knoll, U.; Schartel, B. J Mater Sci Lett 2006, 41, 4981.
24. Von Gentzkow, W.; Huber, J.; Kapitza, H.; Rogler, W. J Vinyl Additive Technol 1997, 3, 175.
25. Levchik, S. V.; Camino, G.; Costa, L.; Luda, M. P. Polym Degrad Stab 1996, 54, 317.
26. Buckingham, M. R.; Lindsay, A. J.; Stevenson, D. E.; Muller, G.; Morel, E.; Costes, B.; Henry, Y. Polym Degrad Stab 1996, 54, 311.
27. Ging-Ho, H.; Liu, Y. L.; Tsiao, J. J. Appl Polym Sci 2000, 78, 1.
28. Preety, J.; Choudhary, V.; Varma, I. K. J Fire Sci 2003, 21, 5.
29. Preety, J.; Choudhary, V.; Varma, I. K. J Appl Polym Sci 2001, 81, 390.
30. Sheng, X. C.; Lin, C. H. J Polym Sci Part A: Polym Chem 2005, 43, 2862.
31. Lin, C. H.; Sheng, X. C.; Lin, C. H. J Polym Sci Part A: Polym Chem 2005, 43, 5971.
32. Wang, C. S.; Lin, C. H. J Appl Polym Sci 1999, 74, 1635.
33. Dörken, C. Chem Ber 1888, 21, 1505.
34. Noyce, D. S.; Virgilio, J A. J Org Chem 1972, 31, 2643.
35. Sukhorukova, N. A.; Baranskii, V. A.; Kalabina, A. V. J Gen Chem USSR 1985, 55, 1670.
36. Streck, R.; Barnes, A. J Spectrochim Acta Part A: Mol Spectrosc 1999, 55, 1049.
37. Soles, C. L.; Chang, F. T.; Gidley, D. W.; Yee, A. F. J Polym Sci Part B: Polym Phys 2000, 38, 776.
38. Prime, R. B. In Thermal Characterization of Polymeric Materials, 2nd ed.; Turi, E. A., Ed.; Academic Press: New York, 1997; Vol. 2, Chapter 6.
39. Chen, Y. S.; Lee, J. S.; Yu, T. L.; Chen, J. C.; Chen, W. Y.; Cheng, M. C. Macromol Chem Phys 1995, 196, 3447.
40. Finzel, M. C.; Delong, J.; Hawley, M. C. J Polym Sci Part A: Polym Chem 1995, 33, 673.
41. Wasserman, S.; Johari, G. P. J Appl Polym Sci 1994, 53, 331.
42. Min, B. G.; Stachurski, Z. H.; Hodgkin, J. H. Polymer 1993, 34, 4488.
43. Lee, J. Y.; Choi, H. K.; Shim, M. J.; Kim, S. W. Thermochim Acta 2000, 343, 111.

44. Paz-Abuin, S.; Pellin, M. P.; Paz-Pazos, M.; Lopez-Quintela, A. Polymer 1997, 38, 3795.
45. Yousefi, A.; Lafleur, P. G.; Gauvin, R. Polym Compos 1997, 18, 157.
46. Varley, R. J.; Hodgkin, J. H.; Hawthorne, D. G.; Simon, G. P. J Appl Polym Sci 1996, 60, 2251.
47. Francis, B.; Poel, G. V.; Posada, F.; Groeninckx, G.; Lakshmana Rao, V.; Ramaswamy, R.; Thomas, S. Polymer 2003, 44, 3687.
48. Jain, P.; Choudhary, V.; Varma, I. K. Eur Polym J 2003, 39, 181.
49. Grillet, A. C.; Galy, J.; Pascault, J. P.; Bardin, I. Polymer 1989, 30, 2094.
50. Flory, P. J. Principles of Polymer Chemistry; Cornel University Press: Ithaca, NY, 1953.
51. Vallo, C. I.; Frontini, P. M.; Williams, R. J. J. J. Polym Sci Part B: Polym Phys 1991, 29, 1503.
52. Meyer, F.; Sanz, G.; Eceiza, A.; Mondragon, I.; Mijovic, J. Polymer 1995, 36, 1407.
53. Varley, R. J.; Heath, G. R.; Hawthorne, D. G.; Hodgkin, J. H.; Simon, G. P. Polymer 1995, 36, 1347.
54. Simon, S. L.; Gillham, J. K. J Appl Polym Sci 1994, 53, 709.
55. Tobolsky, A. V. Properties and Structure of Polymers; Wiley: New York, 1960.
56. LeMay, J. D.; Kelley, F. N. Adv Polym Sci 1986, 78, 115.
57. Johncock, P.; Tudgey, G. F. Br Polym J 1983, 15, 14.
58. Vanlandingham, M. R.; Eduljee, R. F.; Gillespie, J. W., Jr. J Appl Polym Sci 1999, 71, 787.
59. Zhou, J.; Lucas, J. P. Polymer 1999, 40, 5005.
60. Wong, T. C.; Broutman, L. J Polym Eng Sci 1985, 25, 521.
61. Braun, U.; Balabanovich, A. I.; Schartel, B.; Knoll, U.; Artner, J.; Ciesielski, M.; Döring, M.; Perez, R.; Sandler, J. K. W.; Altstädt, V.; Hoffmann, T.; Pospiech, D. Polymer 2006, 47, 8495.
62. Levchik, S. V.; Camino, G.; Luda, M. P.; Costa, L.; Muller, G.; Costes B. Polym Deg Stab 1998, 60, 169.
63. Braun, U.; Knoll, U.; Schartel, B.; Hoffmann, T.; Pospiech, D.; Artner, J.; Ciesielski, M.; Döring, M.; Perez-Graterol, R.; Sandler, J. K. W.; Altstädt, V. Macromol Chem Phys 2006, 7, 1501.
64. Chin, W. K.; Shau, M. D.; Tsai, W. C. J Polym Sci Part A: Polym Chem 1995, 33, 373.
65. Shau, M. D.; Wang, T. S. J Polym Sci Part A: Polym Chem 1996, 34, 387.
66. Wang, C. S.; Shieh, J. Y. Eur Polym J 2000, 36, 443.
67. Lin, J. F.; Ho, C. F.; Huang, S. K. Polym Deg Stab 2000, 67, 137.
68. Wang, Q.; Shi, W. Polym Deg Stab 2006, 91, 1747.
69. Liu, W.; Varley, R. J.; Simon, G. P. Polym Deg Stab 2006, 47, 2091.